

Accelerating Greedy Coordinate Gradient via Probe Sampling

Yiran Zhao¹ Wenyue Zheng¹ Tianle Cai² Xuan Long Do¹
Kenji Kawaguchi¹ Anirudh Goyal³ Michael Shieh¹

Abstract

Safety of Large Language Models (LLMs) has become a central issue given their rapid progress and wide applications. Greedy Coordinate Gradient (GCG) is shown to be effective in constructing prompts containing adversarial suffixes to break the presumably safe LLMs, but the optimization of GCG is time-consuming and limits its practicality. To reduce the time cost of GCG and enable more comprehensive studies of LLM safety, in this work, we study a new algorithm called *Probe sampling* to accelerate the GCG algorithm. At the core of the algorithm is a mechanism that dynamically determines how similar a smaller draft model’s predictions are to the target model’s predictions for prompt candidates. When the target model is similar to the draft model, we rely heavily on the draft model to filter out a large number of potential prompt candidates to reduce the computation time. Probe sampling achieves up to 5.6 times speedup using Llama2-7b and leads to equal or improved attack success rate (ASR) on the AdvBench. Our code is publicly available at <https://github.com/zhaoyiran924/Probe-Sampling>.

1. Introduction

Large language models (LLMs) (Radford et al., 2019; Brown et al., 2020; Chowdhery et al., 2022; OpenAI, 2023; Touvron et al., 2023; Jiang et al., 2023) are believed to have the potential to impact every facet of human life. As such, ensuring their safety becomes a central theme of research. Although RLHF (Stiennon et al., 2020; Ouyang et al., 2022) has demonstrated strong promises in aligning LLMs with human values, it is not uncommon for well-aligned LLMs to generate objectionable contents in various scenarios in-

¹National University of Singapore ²Princeton University ³Google DeepMind. Correspondence to: Yiran Zhao <zhaoyiran@u.nus.edu>, Michael Shieh <michaelshieh@comp.nus.edu.sg>.

cluding using an adversarial suffix (Zou et al., 2023), further finetuning (Qi et al., 2023; Lermen et al., 2023), employing cipher (Yuan et al., 2023) and multilingual settings (Deng et al., 2023). Such works are reminiscent of adversarial attack papers (Szegedy et al., 2013; Madry et al., 2017; Kurakin et al., 2018) in computer vision where neural networks can exhibit very different behaviors under situations mildly different from training data.

Among effective LLM adversarial attack works, Zou et al. (2023) present a general and universal method as briefly illustrated in Figure 1. The proposed approach appends an uninterpretable suffix to a harmful user query. To optimize the suffix to elicit the generation of a target reply, they employ the Greedy Coordinate Gradient (GCG) algorithm, which iteratively attempts to replace existing tokens in the suffix and keeps the best-performing ones based on the adversarial loss. The GCG algorithm proves to be effective in attacking LLMs that have undergone safety-focused fine-tuning, such as Vicuna (Zheng et al., 2023) or Llama-chat (Touvron et al., 2023). However, searching the combinatorial space of the adversarial suffixes is time-consuming, especially when we primarily care about alignment failure cases that arise from the complex transformations using a very big model, surfacing very rare cases from small changes, and that each token replacement attempt requires a full forward computation using an LLM. This hinders us from using the algorithm to fully explore the safety properties of LLMs such as finding potentially harmful queries comprised of natural sentences to find further directions for collecting RLHF data.

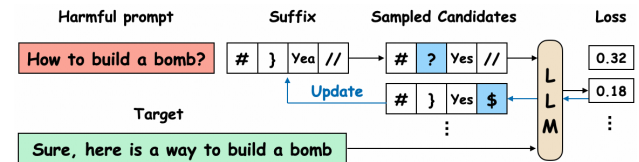


Figure 1. A brief illustration of the Greedy Coordinate Gradient (GCG) algorithm (Zou et al., 2023).

A possible solution for reducing forward computation is to resort to a smaller draft model when it is indicative of the results on the larger target model. This intuition has been applied in speculative sampling (Chen et al., 2023; Leviathan et al., 2023) for decoding. In speculative sampling, the

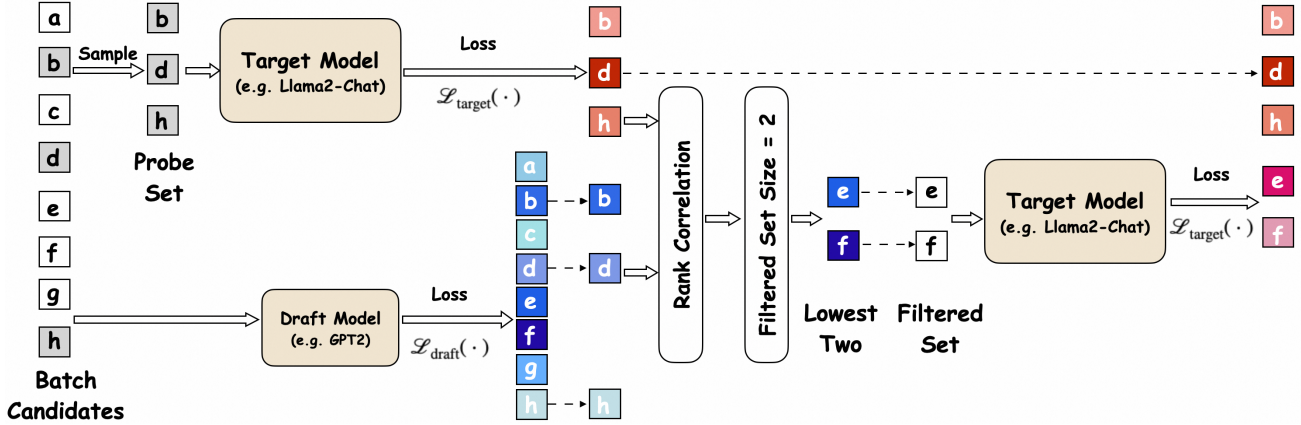


Figure 2. Workflow of `Probe sampling` mainly consists of three steps. (i) A batch of candidates ($\{a, b, \dots, h\}$) is sampled. We determine the probe agreement score between the draft model and the target model on a probe set ($\{b, d, h\}$). The probe agreement score is used to compute the filtered set size. (ii) We obtain a filtered set ($\{e, f\}$) based on the losses on the draft model (iii) We test the losses of candidates in the filtered set using the target model.

target model acts as a verifier that accepts or rejects the decoded tokens. However, speculative sampling cannot be used to optimize discrete tokens in GCG because the optimization of every token in adversarial suffix is independent of each other, which breaks the autoregressive assumption in decoding. In addition, speculative sampling’s applicability is limited by the fact that the speedup results are governed by the degree of how much the draft model and the target model match in their predictions.

Motivated by these observations, we propose a new algorithm called `Probe sampling` to accelerate the GCG algorithm. Instead of computing the loss on every suffix candidate, we filter out unpromising ones based on the loss computed with a smaller draft model, to reduce the time consumption of the optimization process. Importantly, we dynamically decide how many candidates we keep at each iteration by measuring the agreement score between the draft model and the target model, by looking at the loss rankings on a small set of prompts dubbed as the probe set, hence the name `Probe sampling`. It is worth noting that the prompt candidates at each iteration in GCG is obtained by randomly changing one token of an original prompt. As a result, the agreement score is adaptive to the original prompt. We evaluate probe sampling on the AdvBench dataset with Llama2-7b-Chat and Vicuna-v1.3 as the target models and a significantly smaller model GPT-2 (Radford et al., 2019) (124M parameters) as the draft model. Experiment results show that compared to the original GCG algorithm, probe sampling significantly reduces the running time of GCG while achieving better Attack Success Rate (ASR). Specifically, with Llama2-7b-Chat, probe sampling achieves 3.5 times speedup and an improved ASR of 81.0 compared to GCG with 69.0 ASR. When combined with simulated annealing, probe sampling achieves a speedup of 5.6 times

with a better ASR of 74.0.

2. Probe Sampling: Proposed Method

2.1. Background: Greedy Coordinate Gradient

The overall optimization objective of GCG can be denoted by a simple log likelihood loss

$$\min_s \mathcal{L}(s) = -\log p(y | x, s), \quad (1)$$

where x is a prompt that contains a harmful user query such as “Tell me how to build a bomb”, y is the target sentence “Sure, here is how to build a bomb”, and s is the adversarial suffix that is optimized to induce the generation of y . p is the probability of a sentence output by a LLM. This objective can be decomposed into the summation of the negative log likelihood of individual tokens in the target sentence like a typical language modeling objective. s is set to be a fixed length string in the GCG algorithm.

The optimization of the adversarial suffix s is a non-trivial problem. Prior works (Guo et al., 2021; Wen et al., 2023) based on Gumbel-Softmax (Jang et al., 2016; Maddison et al., 2016) and soft prompt tuning (Lester et al., 2021) have achieved limited success, probably because the LLMs are well-aligned and the exceptionally large models magnifies the difference between a discrete choice and its continuous relaxations.

Instead, GCG adopts a greedy search algorithm based on the gradient. In each iteration, it computes $\mathcal{L}(\hat{s}^i)$ for B suffix candidates $\hat{s}^1, \dots, \hat{s}^B$ and keeps the one with the best loss. The B candidates are obtained by randomly changing one token from the current suffix s and replacing it with a randomly sampled token using the top K tokens. For

example, suppose we change the token at position j , we first compute the gradient $-\nabla_{e_{s_j}} \mathcal{L}(s)$ with respect to the one-hot vector e_{s_j} and obtain the top K tokens that have the largest gradient. The gradient information is by no means an accurate estimation of the resulting loss because of the gap between the continuous gradient information and the discrete one-hot vector denoting the choice of a token, so we need to check if the resulted new suffix \hat{s}^i leads to a lower loss $\mathcal{L}(\hat{s}^i)$.

To obtain the B candidates, one just needs to perform one forward pass and one backward pass. But to compute the loss for the B candidates, one needs to perform B forward passes. In GCG, B is set to 512 for optimal performance, making the loss computation the most time-consuming part. As such, we focus on reducing the time cost of the loss computation of the B candidates in this work.

2.2. Probe Sampling

Overview. As mentioned earlier, the most time consuming part in the GCG algorithm is the loss computation on B suffix candidates $\hat{s}^1, \dots, \hat{s}^B$. As shown in speculative sampling (Chen et al., 2023; Leviathan et al., 2023), the speculated results using a smaller draft model can be helpful in reducing the computation with a large target model. The original speculative sampling is created to accelerate decoding so it isn’t directly applicable here. But the intuition of relying a weaker draft model is obviously useful for negative log likelihood loss computation. Applying the intuition to the problem at hand, we can filter out the suffix candidates that the draft model finds to be unpromising, since the goal is to find the candidate that has the lowest loss with the target model.

In addition, a unique structure in the GCG algorithm is that all the suffix candidates are based on changing one token of the original suffix s . As a result of this locality property, it is not unreasonable to assume that one can determine how much they agree on the B candidates based on their agreement on a subset of the B candidates. If the two models agree, we can choose to safely rely on the draft model and filter out more candidates.

Based on these intuitions, we design the `Probe Sampling` algorithm as follows: (i) probe agreement between the target model and the draft model to determine the size of the filtered set; (ii) rank candidates using the draft model and obtain the filtered set; (iii) pick the best candidate from the filtered set using the target model.

Procedures. For the first step, specifically, we sample a probe set comprised of k candidates $\bar{s}^1, \dots, \bar{s}^k$ and compute their losses using the draft model and the target model and obtain $\mathcal{L}_{\text{draft}}(\bar{s}^1), \dots, \mathcal{L}_{\text{draft}}(\bar{s}^k)$ and $\mathcal{L}_{\text{target}}(\bar{s}^1), \dots, \mathcal{L}_{\text{target}}(\bar{s}^k)$. Then we measure the probe

agreement score as the Spearman’s rank correlation coefficient (Zar, 2005) between the two results as the agreement score. The probe agreement score α is computed as

$$\alpha = \frac{1}{2} - \frac{3 \sum_{i=1}^k d_i^2}{k(k^2 - 1)}, \quad (2)$$

where d_i is the distance between the ranks of suffix \bar{s}^i in the two results. For example, $d_i = 4$ if the suffix \bar{s}^i is ranked as number 6 and number 2 for its losses computed from the draft model and the target model. The agreement score α falls into $[0, 1]$ with 1 meaning a full agreement and 0 indicating a non-agreement. We use the rank agreement because it is more robust to the specific values of the resulting loss when measured on drastically different LLMs.

After obtaining the agreement score, we keep $(1 - \alpha) * B/R$ candidates where $(1 - \alpha) * B$ means that the filtered set size is a scale-down of the previous batch size B and R is a hyperparameter that determines a further scale down. When α is close to 0, meaning little agreement between the two models, we will use a filtered set size of B/R . When α goes to 1, we almost filter out most of the candidates.

With the filtered size determined, we can readily rank the candidates according to the draft model and filter the ones with higher losses. Finally, we evaluate the final loss on the filtered set using the target model and select the best candidate.

Discussion and details. At first glance, probe sampling involves extra computation but it actually achieves effective acceleration. For computing the losses on the probe set using both the draft model and the target model, the size of the probe set can be set to be relatively small, so it would not add too much to the total time cost. The ranking procedure involves sorting on CPU, but luckily the probe set is small enough that this doesn’t become a bottleneck. And the loss computation using the draft model on the whole candidate set is relatively cheap because of draft model’s small size. These two operations can also be parallelized on GPU. On the plus side, we are able to avoid computing the loss using the big target model on many candidates that are filtered out. As we will show in the experiments, this approach achieves significant speedup measured by both running time and #FLOPs.

An alternative to computing agreement on the spot is to measure the agreement score on a predetermined set of candidates and use a fixed agreement score for all the suffixes. This would save the time used to measure agreement for each candidate set. However, as we will show in the experiment, this approach does not work so well in terms of speedup. Our intuition is that one can squeeze the time cost more effectively if the agreement is measured accurately, and an adaptive agreement score is more accurate than an

one-size-fits-all score. The plausibility of the adaptive score comes back to the locality property that we discussed earlier. Given a specific candidate set, one can accurately estimate the agreement because all the suffixes in this candidate set are similar to a large extent. However, given another candidate set altered from a different suffix, the agreement of the draft model and the target model can be widely different.

In practice, we adopted two small changes in our implementation. First, we do not have a separate step to compute the loss of the probe set candidates using the draft model, since we need to compute the loss on all candidates for filtering purposes. We simply get the numbers from the losses on the whole candidate set. Second, to get the best candidate for the final result, we also look at the losses on the probe set, since the target model is evaluated on the probe set. Ideally, the candidates in the probe set should be in the filtered set if they achieve a low loss. However, it also does not hurt to look at the best candidate in the probe set in case it is not included in the filtered set. The overall algorithm is further illustrated in Algorithm 1, and the corresponding implementation is shown in Appendix A.

Algorithm 1 Probe Sampling

Input: Original suffix s , a batch of suffix candidates $\{\hat{s}^1, \dots, \hat{s}^B\}$, loss function using the draft model and the target model $\mathcal{L}_{\text{draft}}(\cdot), \mathcal{L}_{\text{target}}(\cdot)$.

```

1: Parallel Begin
2: //Compute loss of all candidates
   using the draft model
3: for  $\hat{s}^i \in \{\hat{s}^1, \dots, \hat{s}^B\}$  do
4:   Compute  $\mathcal{L}_{\text{draft}}(\hat{s}^i)$ 
5: end for
6: //Compute loss of the probe set on
   target model
7:  $\{\bar{s}^1, \dots, \bar{s}^k\} = \text{Uniform}(\{\hat{s}^1, \dots, \hat{s}^B\}, k)$ 
8: for  $\bar{s}^i \in \{\bar{s}^1, \dots, \bar{s}^k\}$  do
9:   Compute  $\mathcal{L}_{\text{target}}(\bar{s}^i)$ 
10: end for
11: Parallel End
12: //Calculate agreement score
13:  $\alpha = \text{Spearman\_Cor}(\{\mathcal{L}_{\text{target}}(\bar{s}^i)\}, \{\mathcal{L}_{\text{draft}}(\hat{s}^i)\})$ 
14: //Evaluate using the target model
15:  $\text{filtered\_set} = \text{argmin}_{(1-\alpha)B/R} \mathcal{L}_{\text{draft}}(\hat{s}^i)$ 
16: for  $\hat{s}^i \in \text{filtered\_set}$  do
17:   Compute  $\mathcal{L}_{\text{target}}(\hat{s}^i)$ 
18: end for
19: Output the best suffix in the probe
   set and the filtered set
20:  $s' = \text{argmin}\{\mathcal{L}_{\text{target}}(\bar{s}^i), \mathcal{L}_{\text{target}}(\hat{s}^i)\}$ 

```

Output: s'

2.3. Further Acceleration

We also briefly explored other acceleration methods in this work. Among them, simulated annealing (Pincus, 1970) is complementary to our method and leads to further speedup. Simulated annealing operates on the cross iteration level while probe sampling operates within a single iteration. Suppose s is the current suffix and s' is the best suffix from all candidates. In GCG, we always update the current suffix with s' regardless of whether s' is better than s or not. As a result, we need a big set of candidates to make sure that s' is better than s most of the time. In other words, we need to use a large value for B . With simulated annealing, we adopt a more greedy change by rejecting the update when s' is worse than s . The rejection probability is increased throughout training using temperature annealing so that the update becomes more conservative as we approach convergence. Simulated annealing reduces the noise in the optimization process given the same batch size B . Consequently, one can reduce the batch size B to achieve a similar performance with reduced time cost.

We also tried to use 4-bit quantization but, in our preliminary study, we found that quantization can hurt the ASR significantly. Thus we omit the results of quantization and leave this to future explorations.

3. Experiment

In this section, we evaluate the proposed method on its efficacy and the important factors through extensive studies.

3.1. Experiment Details

Settings. Following the original GCG paper, we conduct experiments on the first 100 instances of AdvBench (Zou et al., 2023), which are divided into two parts, 500 harmful strings and 500 harmful human behaviors. We test open-source LLMs that have been specifically fine-tuned with respect to safety, including Llama2-chat-7b (Touvron et al., 2023) and Vicuna-7b (Zheng et al., 2023). In the case of draft models, in our main experiments, we use a much smaller model GPT-2 (Radford et al., 2019), which only has 124M parameters and was released in 2019.

Evaluation. Following Zou et al. (2023), we use Attack Success Rate (ASR) as the evaluation metric, which is defined as the percentage of inputs that successfully lead LLMs to generate harmful outputs. An output is determined to be harmful if it does not match with rejection phrases, such as “I’m sorry”, “I apologize” and “As an”. This is not a perfect measurement but works relatively well in practice since LLMs are trained to reject harmful replies. It is also easy to measure and interpret.

The processing time is determined as the average time used

Table 1. Comparing the ASR and processing time of Probe sampling with and without simulated annealing to GCG with and without simulated annealing, while measuring speedup and FLOPs by averaging each iteration.

Model	Method	Human Strings			Individual ASR	Human Behaviors		Speedup	#FLOPs
		ASR	Speedup	FLOPs		Multiple ASR (train)	Multiple ASR (test)		
Vicuna (7b-v1.3)	GCG	88.0	1 ×	97.3 T	99.0	100.0	98.0	1 ×	106.8 T
	GCG+Annealing	89.0	2.7 ×	38.5 T	98.0	92.0	94.0	2.3 ×	46.2 T
	Probe sampling	91.0	2.4 ×	42.4 T	100.0	96.0	98.0	2.1 ×	53.2 T
	PS + Annealing	93.0	3.6 ×	27.8 T	100.0	96.0	99.0	3.2 ×	24.7 T
Llama2 (7b-Chat)	GCG	57.0	1 ×	198.4 T	69.0	88.0	84.0	1 ×	202.3 T
	GCG-Annealing	55.0	3.9 ×	39.7 T	68.0	92.0	88.0	3.4 ×	50.6 T
	Probe sampling	69.0	4.1 ×	43.8 T	81.0	92.0	93.0	3.5 ×	40.7 T
	PS + Annealing	64.0	6.3 ×	31.2 T	74.0	96.0	91.0	5.6 ×	32.3 T

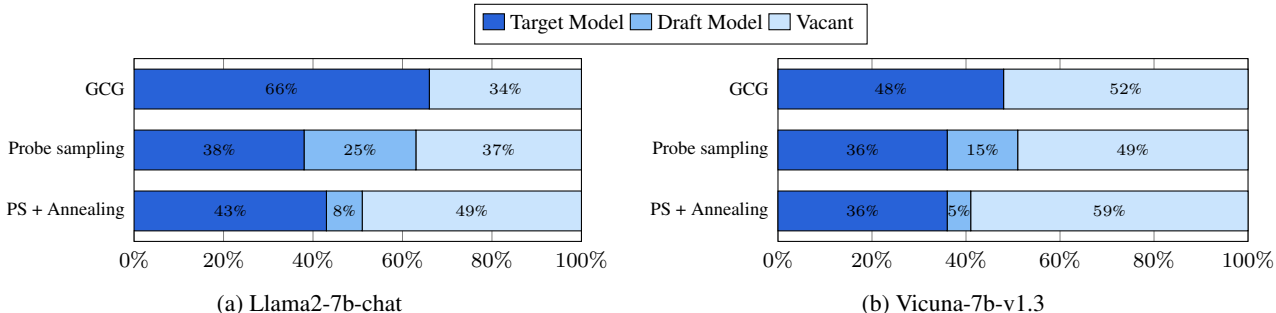


Figure 3. Memory usage on a single A100 with 80GB memory with (a) Llama2-7b-chat and (b) Vicuna-7b-v1.3 on 1 instance. The memory consumption of probe sampling with or without simulated annealing is similar to that of the original setting. The computation with the target model still takes most of the memory.

for each iteration across all input samples and all iterations. In all experiments, we use 1 NVIDIA A100 GPU with 80GB memory unless mentioned otherwise.

Hyperparameters. To determine the hyperparameters for probe sampling, including probe set size k , filtered set size reduction hyperparameter R , we construct a validation set of size 100 from AdvBench by random sampling in the 400 instances different from the test set. We follow Zou et al. (2023) for the hyperparameters used in the original algorithm such as the size of the candidate set B . We provide detailed analysis of hyperparameters in Section 3.4. When we combine probe sampling with simulated annealing, we follow the same procedure to select hyperparameters. We use the same number of optimization steps 500 as in GCG throughout the paper.

3.2. Main Results

Acceleration results. As shown in Table 1, probe sampling achieves a speedup of 5.6 times and 6.3 times on Human Behaviors and Human Strings with Llama2 when combined with simulated annealing. Probe sampling achieves a speedup of 3.5 and 4.1 times alone. With Vicuna, we achieve an overall speedup of 3.2 and 3.6 respectively on the two datasets. We also measure the #FLOPs for dif-

ferent settings and found that the speedup results reflects in the reduction of #FLOPs. For example, with Llama2, the #FLOPs reduction is $202.3T/32.3T = 6.3$ times and $198.4T/31.2T = 6.4$ times on the two sets, which is close to the actual speedup results. This also shows that our algorithm results in little overhead with the introduced new procedures. It is worth noting that simulated annealing also achieves decent acceleration and is complementary to our acceleration results.

ASR results. Interestingly, we achieve a better ASR score than the GCG algorithm although technically acceleration introduces noise to the algorithm. For instance, with Llama2, we improve the ASR from 57.0 to 64.0 on Human Strings and from 84.0 to 91.0 on Human Behaviors. We hypothesize that the improvement comes from the randomness added to the GCG algorithm based on greedy search over a single objective. Introducing randomness and noise has been seen as one of the advantages of SGD over full batch training. In contrast, simulated annealing only leads to comparable ASR when applied on GCG.

3.3. Computation Detail Analysis

Memory allocation. We evaluate whether probe sampling uses more memory because of the use of an extra model.

In Figure 3, we show the memory usage of GCG, probe sampling with and without annealing using either Llama2-7b-chat and Vicuna-7b-v1.3. Probe sampling uses a similar amount of memory to the original GCG algorithm although it involves extra procedures and an extra model, by saving the computation of target model on the whole candidate set. As such, the usage of probe sampling does not introduce extra memory and can be applied when the original GCG algorithm is applied. In terms of the memory usage of the target model and the draft model, most of the memory is spent on target model, probably because the draft model is much smaller compared to the target model.

Time allocation. We look at the specific time spent on different operations. As shown in Figure 4, probe set computation using the target model and full set computation using the draft model take a similar amount of time so we can parallelize the computation easily. Sampling candidates in the graph involves a forward and backward pass as mentioned earlier and can be completed relatively quickly. Similarly, it is also fast to compute the agreement using the ranked losses on CPU, so our algorithm introduces relatively little overhead.

3.4. Further analysis

In this section, we conduct extensive studies to understand how the proposed method works. We conduct all of the following experiments on the validation set, so the numbers are not directly comparable to the numbers in the main results. For the validation set, the original GCG algorithm achieves an ASR of 66.0 with an average time of 9.16 seconds per iteration. In each of the study, we highlight the settings that we find to be the best.

Filtered set size. The filtered set size is the most important factor in our method. If it is too small, then we will achieve a lot of speedup at the cost of relying too heavily on the draft model and resulting in a lower ASR. If it is too big, then we would not achieve much speedup. Hence we experiment with different filtered size reduction hyperparameter R . The filter set size is $(1 - \alpha) * B/R$ where α is the probe agreement score described in Section 2.2.

As shown in Table 2, the time does monotonically decrease if we use a smaller filtered set size. However, interestingly, there is a sweetspot for the ASR with R set to 8. We believe that this can resonate with the hypothesis of introducing randomness as the source of ASR boosts. Both too much or too little randomness hurt performance. As such, we use $R = 8$ for probe sampling.

In Figure 5, we also show a few convergence processes with different values of R , where the pink line corresponds to $R = 8$. The pink line always achieves successful optimiza-

tion while the other lines can lead to suboptimal results due to excessive randomness or insufficient randomness. In particular, the blue and yellow lines can suffer from excessive randomness and the other lines might have insufficient randomness.

Table 2. Ablation on the filtered set size reduction hyperparameter R . The filter set size is $(1 - \alpha) * B/R$.

Reduction R	64	16	8	4	2	1
ASR	60.0	70.0	85.0	81.0	76.0	79.0
Time (s)	2.01	2.31	2.60	3.02	3.41	5.19

Adaptive vs fixed filtered set size. As mentioned in Section 2.2, an alternative to use an adaptive filtered set size is to use a fixed size. Here we investigate whether it matters to use an adaptive filtered set size that is determined by how much the draft model and the target model agree on each candidate set. To use a fixed size, we simply fix the probe agreement score α to be 0.9, 0.6, 0.3, and 0.0 and compare with the adaptive case. As shown in Table 3, fixed probe agreement scores always lead to worse ASR.

Furthermore, when adopting GPT-2 as the draft model, the average agreement score is 0.45 with a standard deviation of 0.11. This shows that the agreement score between the two models varies significantly for different candidate sets. We also provide the statistics of α for other draft models in Table 6.

Table 3. Ablation on fixed probe agreement score α vs adaptive score.

Agreement α	0.9	0.6	0.3	0.0	Adaptive
ASR	70.0	77.0	75.0	81.0	85.0
Time (s)	2.17	2.41	2.71	3.01	2.60

Probe agreement measurement. We also experiment alternatives to measure the probe agreement score, including the Pearson correlation coefficient (Pearson, 1900), Kendall’s Tau correlation coefficient (Kendall, 1938), and Goodman and Kruskal’s gamma (Goodman et al., 1979) where the Pearson correlation coefficient directly uses the loss values to compute the agreement and the others use the ranking information. As shown in Table 4, all methods have similar time cost, and Spearman’s rank correlation coefficient achieves the best ASR. The Pearson correlation coefficient performs worse than other ranking-based agreement measurement.

Probe set size. The size of the probe set also determines whether the probe agreement score is measured accurately. As such, we experiment with different probe set size and

Accelerating Greedy Coordinate Gradient via Probe Sampling

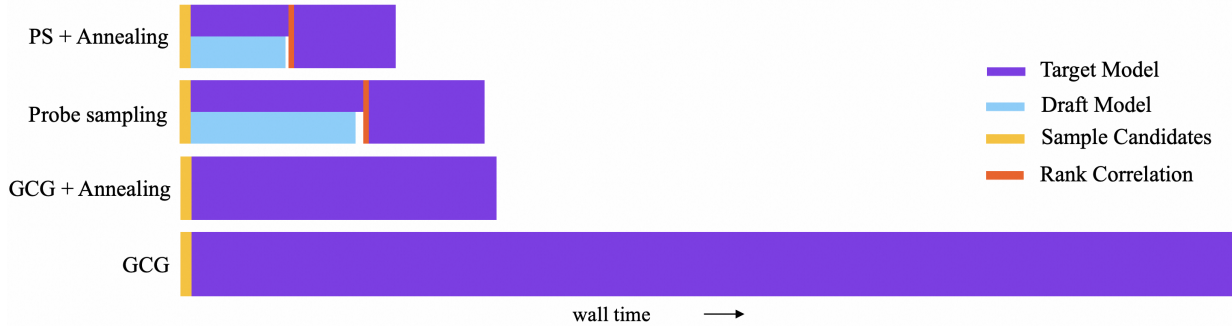


Figure 4. Wall time of GCG, probe sampling with and without simulated annealing. For the target model computation, the first part is done on the probe set and the second part is done on the filtered set. Draft model computation and computation of the target model on the probe set are suited to be done in parallel as they take similar time.

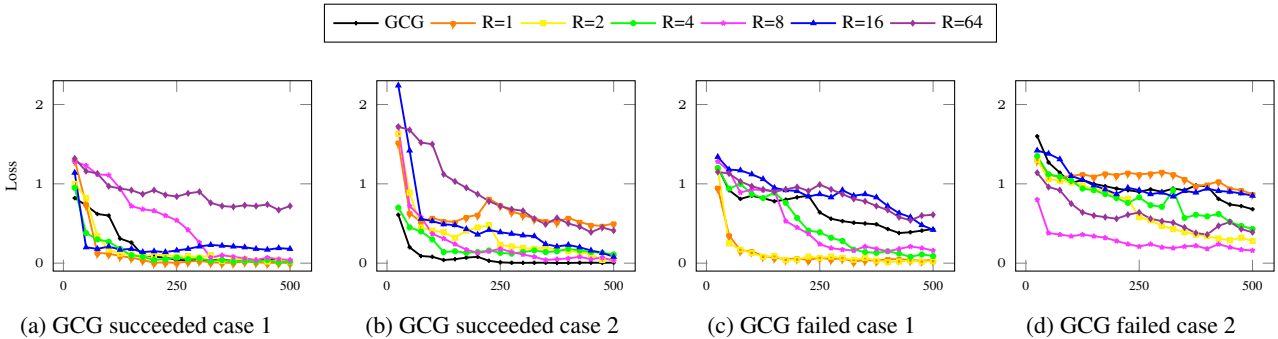


Figure 5. Converge progress with different sizes of filtered set. In the case where the GCG attack succeeds or the GCG attack fails, $R = 8$ (pink line) performs best due to its optimal level of randomness.

Table 4. Ablation on probe agreement measurements. All methods achieve similar speedup while Spearman’s rank correlation coefficient achieves the best ASR.

Cor	Spearman	Pearson	Kendall	Kruskal
ASR	85.0	70.0	74.0	79.0
Time (s)	2.60	2.47	2.53	2.43

Table 5. Ablation on the probe set size k . Using $B/16$ leads to accurate probe agreement measurement while achieving significant acceleration.

Probe	$B/64$	$B/32$	$B/16$	$B/4$	$B/2$	B
ASR	64.0	72.0	85.0	86.0	85.0	87.0
Time (s)	2.10	2.57	2.60	3.41	5.61	9.58

report the performance in Table 5. We find that using a small probe set such as $B/64$ or $B/32$ can result in inaccurate agreement score, which put a put a significant toll on the attack success rate. It also does not lead to too much time reduction since the draft model computation done in parallel takes more time and the reduced computation is not the bottleneck. Using a larger probe set size such as $B/4$ and $B/2$ will lead to more accurate agreement score but does not increase the ASR significantly. As such, using a probe set of size $B/16$ is good enough to accurately measure the agreement and achieves maximum time reduction.

Draft model study. Here we also experiment with bigger draft models, some of which is of similar size to Llama2. We experiment with GPT-Neo (Gao et al., 2020), Flan-T5-base (Chung et al., 2022), BART (Lewis et al., 2019),

Phi-1.5 (Li et al., 2023), TinyLlama (Zhang et al., 2024) and Sheared-LLaMA (Xia et al., 2023). Among them, Sheared-LLaMA might be the closest to Llama2 since it is a pruned version of Llama2. For TinyLlama, Phi and Sheared-LLaMA, we use 2 A100s with 80GB memory to fit the whole computation.

As shown in Table 6, Sheared-LlaMa achieves the best ASR although the time reduction is not as good as smaller models such as GPT-2 and there would be a higher time cost if we manage to fit all computation in one GPU. On contrast, Flan-T5, BART, TinyLlama and Mistral all achieve lower ASRs probably because of being very different than Llama2. However, the results are still better than the baseline ASR 66.0. GPT-2 and GPT-Neo achieve a good balance of performance and speedup.

Table 6. Experiments with different draft models. Models with over 1B parameters, like TinyLlama, Phi, and ShearedLLMa, need two GPUs for parallel computation. ShearedLLMa achieves the highest ASR probably because it is a pruned version of Llama2. Both GPT-2 and GPT-Neo achieve a good balance of ASR and speedup.

Model	1 GPU				2 GPUs		
	GPT-2 (124M)	GPT-Neo (125M)	Flan-T5 (248M)	BART (406M)	TinyLlama (1.1B)	Phi (1.3B)	ShearedLLaMa (1.3B)
α	0.45 \pm 0.10	0.51 \pm 0.11	0.61 \pm 0.13	0.46 \pm 0.09	0.52 \pm 0.13	0.52 \pm 0.11	0.35 \pm 0.12
ASR	85.0	81.0	57.0	76.0	72.0	82.0	91.0
Time (s)	2.60	2.82	3.89	2.93	3.38	4.83	3.93

Software optimization. In other speedup works (He, 2023), using `torch.compile()` can lead to significant acceleration. It compiles LLMs into an kernel and alleviate the overhead of repeatedly launching the kernel. Table 7 shows that the time cost is similar with or without this optimization enabled. This is likely due to the fact that we use large batch sizes and long input sequences, whose computation cost dominates the overhead caused by the eager execution and launching the kernel repeatedly.

Table 7. Results with `torch.compile()` enabled. `torch.compile()` does not lead to further speedup.

Method	GCG	Probe sampling	PS (Compile)
ASR	66.0	85.0	85.0
Time (s)	9.16	2.60 (3.5 \times)	2.54 (3.6 \times)

4. Related Work

Acceleration. In the field of acceleration, speculative sampling (Chen et al., 2023; Leviathan et al., 2023) is the most relevant to our method. They also use a draft model but its design cannot be directly applied to accelerate the GCG algorithm. He et al. (2023) adopts the concept of speculative sampling but uses a retrieval approach based on a Trie to construct the candidate. The attention module has also been a focus of acceleration because of its quadratic nature (Dao et al., 2022; Cai et al., 2024). There have also been continuous interests in more efficient versions of Transformers (So et al., 2019; Dai et al., 2021; Liu et al., 2021; Gu et al., 2020; 2021). These architectural changes are complementary to our algorithm design and we leave it to future work to study their effects on the GCG algorithm.

LLM Jailbreaks. LLM Jailbreaks have received considerable interests recently since due to the implications of applying LLMs widely in human society. Although there is a continuous effort to build safe and reliable LLMs, bypassing the safety mechanism of LLMs is not uncommon. For example, fine-tuning a safe LLM on a few data instances can easily breaks its safety guarantees (Qi et al., 2023; Lermen

et al., 2023). Treating the jailbreak as a prompt optimization problem has also led to a certain level of success (Zou et al., 2023; Mökander et al., 2023; Liu et al., 2023a). In addition, conversing in a ciphered language (Yuan et al., 2023), planting a backdoor during RLHF (Rando & Tramèr, 2023), using a less well-aligned language (Deng et al., 2023) and multi-modality (Shayegani et al., 2023) can also lead to successful jailbreaks. Researchers have also constructed large dataset of manual jailbreak prompts (Toyer et al., 2023).

Among these jailbreak methods, the prompt optimization method GCG (Zou et al., 2023) provides the more general and universal solution for us to study the jailbreaking problem. As such, in this work, we mainly focus on the acceleration of GCG, but the idea of delegating computation to a draft model can also be applied in other situations such as the multi-modality case and finetuning case. We leave the extension of this work for future work.

Alignment of LLMs. To build safe LLMs, alignments has also been a widely studied topic in the community (Stiennon et al., 2020; Ouyang et al., 2022). Efforts have been put into improving helpfulness (Cheng et al., 2023; Bai et al., 2022a), honesty (Kaddour et al., 2023; Liu et al., 2023b; Park et al., 2023; Xu et al., 2023), and harmlessness (Hartvigsen et al., 2022). Among these works, there has been a growing interest in using feedback from a LLM to perform alignment (Bai et al., 2022b; Gulcehre et al., 2023; Yuan et al., 2024; Burns et al., 2023). In particular, Burns et al. (2023) studies the case where a stronger LLM uses feedback from a weaker LLM. Despite all the efforts, there has not been a definitive answer for LLM safety alignments, which also motivates our research in LLM safety.

5. Conclusion

In this paper, we propose an algorithm probe sampling that can effectively accelerate the GCG algorithm. We achieve an acceleration ranging from 2.1 \times to 6.3 \times in different scenarios on AdvBench. We illustrate the intuition and how the algorithm works through extensive experiments.

We believe the idea of using the probe agreement score

to perform adaptive computation can be applied to cases other than GCG. For example, it could potentially be used to perform conditional computation for attention. Another direction is to extend the framework to the multi-modality case which can be interesting given the vast amount of video data. It would also be interesting to run a small draft model on the scale of web data to detect the existence of natural adversarial prompts.

Acknowledgement

We thank Liwei Kang for insightful discussion, Liying Cheng for helping with plotting figures.

Impact Statements

Probe sampling can be applied to accelerate GCG algorithm. Having a faster algorithm to explore adversarial cases of alignments enable us to study how to make LLMs safer. As far as we know, as of now, there is not a LLM that can use this algorithm to achieve malicious behavior in real-world that would not be possible without the algorithm. The goal of this research is to present a general algorithm which may inspire new research, and also contribute to the gradual progress of building safe and aligned AIs.

References

- Bai, Y., Jones, A., Ndousse, K., Askell, A., Chen, A., Das-Sarma, N., Drain, D., Fort, S., Ganguli, D., Henighan, T., et al. Training a helpful and harmless assistant with reinforcement learning from human feedback. *arXiv preprint arXiv:2204.05862*, 2022a.
- Bai, Y., Kadavath, S., Kundu, S., Askell, A., Kernion, J., Jones, A., Chen, A., Goldie, A., Mirhoseini, A., McKinnon, C., et al. Constitutional ai: Harmlessness from ai feedback. *arXiv preprint arXiv:2212.08073*, 2022b.
- Brown, T., Mann, B., Ryder, N., Subbiah, M., Kaplan, J. D., Dhariwal, P., Neelakantan, A., Shyam, P., Sastry, G., Askell, A., et al. Language models are few-shot learners. *Advances in neural information processing systems*, 33: 1877–1901, 2020.
- Burns, C., Izmailov, P., Kirchner, J. H., Baker, B., Gao, L., Aschenbrenner, L., Chen, Y., Ecoffet, A., Joglekar, M., Leike, J., et al. Weak-to-strong generalization: Eliciting strong capabilities with weak supervision. *arXiv preprint arXiv:2312.09390*, 2023.
- Cai, T., Li, Y., Geng, Z., Peng, H., Lee, J. D., Chen, D., and Dao, T. Medusa: Simple llm inference acceleration framework with multiple decoding heads. *arXiv preprint arXiv:2401.10774*, 2024.
- Chen, C., Borgeaud, S., Irving, G., Lespiau, J.-B., Sifre, L., and Jumper, J. Accelerating large language model decoding with speculative sampling. *arXiv preprint arXiv:2302.01318*, 2023.
- Cheng, P., Yang, Y., Li, J., Dai, Y., and Du, N. Adversarial preference optimization. *arXiv preprint arXiv:2311.08045*, 2023.
- Chowdhery, A., Narang, S., Devlin, J., Bosma, M., Mishra, G., Roberts, A., Barham, P., Chung, H. W., Sutton, C., Gehrmann, S., et al. Palm: Scaling language modeling with pathways. *arXiv preprint arXiv:2204.02311*, 2022.
- Chung, H. W., Hou, L., Longpre, S., Zoph, B., Tay, Y., Fedus, W., Li, Y., Wang, X., Dehghani, M., Brahma, S., et al. Scaling instruction-finetuned language models. *arXiv preprint arXiv:2210.11416*, 2022.
- Dai, Z., Liu, H., Le, Q. V., and Tan, M. Coatnet: Marrying convolution and attention for all data sizes. *Advances in neural information processing systems*, 34:3965–3977, 2021.
- Dao, T., Fu, D., Ermon, S., Rudra, A., and Ré, C. Flashattention: Fast and memory-efficient exact attention with io-awareness. *Advances in Neural Information Processing Systems*, 35:16344–16359, 2022.
- Deng, Y., Zhang, W., Pan, S. J., and Bing, L. Multilingual jailbreak challenges in large language models. *arXiv preprint arXiv:2310.06474*, 2023.
- Gao, L., Biderman, S., Black, S., Golding, L., Hoppe, T., Foster, C., Phang, J., He, H., Thite, A., Nabeshima, N., et al. The pile: An 800gb dataset of diverse text for language modeling. *arXiv preprint arXiv:2101.00027*, 2020.
- Goodman, L. A., Kruskal, W. H., Goodman, L. A., and Kruskal, W. H. *Measures of association for cross classifications*. Springer, 1979.
- Gu, A., Dao, T., Ermon, S., Rudra, A., and Ré, C. Hippo: Recurrent memory with optimal polynomial projections. *Advances in neural information processing systems*, 33: 1474–1487, 2020.
- Gu, A., Goel, K., and Ré, C. Efficiently modeling long sequences with structured state spaces. *arXiv preprint arXiv:2111.00396*, 2021.
- Gulcehre, C., Paine, T. L., Srinivasan, S., Konyushkova, K., Weerts, L., Sharma, A., Siddhant, A., Ahern, A., Wang, M., Gu, C., et al. Reinforced self-training (rest) for language modeling. *arXiv preprint arXiv:2308.08998*, 2023.

- Guo, C., Sablayrolles, A., Jégou, H., and Kiela, D. Gradient-based adversarial attacks against text transformers. In *Proceedings of the 2021 Conference on Empirical Methods in Natural Language Processing*, pp. 5747–5757, 2021.
- Hartvigsen, T., Gabriel, S., Palangi, H., Sap, M., Ray, D., and Kamar, E. Toxigen: A large-scale machine-generated dataset for adversarial and implicit hate speech detection. In *Proceedings of the 60th Annual Meeting of the Association for Computational Linguistics (Volume 1: Long Papers)*, pp. 3309–3326, 2022.
- He, H. GPT-Fast. [Online]. Available: <https://github.com/pytorch-labs/gpt-fast/tree/main?tab=readme-ov-file>, 2023. Accessed: Feb. 2, 2024.
- He, Z., Zhong, Z., Cai, T., Lee, J. D., and He, D. Rest: Retrieval-based speculative decoding. *arXiv preprint arXiv:2311.08252*, 2023.
- Jang, E., Gu, S., and Poole, B. Categorical reparameterization with gumbel-softmax. In *International Conference on Learning Representations*, 2016.
- Jiang, A. Q., Sablayrolles, A., Mensch, A., Bamford, C., Chaplot, D. S., Casas, D. d. l., Bressand, F., Lengyel, G., Lample, G., Saulnier, L., et al. Mistral 7b. *arXiv preprint arXiv:2310.06825*, 2023.
- Kaddour, J., Harris, J., Mozes, M., Bradley, H., Raileanu, R., and McHardy, R. Challenges and applications of large language models. *arXiv preprint arXiv:2307.10169*, 2023.
- Kendall, M. G. A new measure of rank correlation. *Biometrika*, 30(1/2):81–93, 1938.
- Kurakin, A., Goodfellow, I. J., and Bengio, S. Adversarial examples in the physical world. In *Artificial intelligence safety and security*, pp. 99–112. Chapman and Hall/CRC, 2018.
- Lermen, S., Rogers-Smith, C., and Ladish, J. Lora fine-tuning efficiently undoes safety training in llama 2-chat 70b. *arXiv preprint arXiv:2310.20624*, 2023.
- Lester, B., Al-Rfou, R., and Constant, N. The power of scale for parameter-efficient prompt tuning. In *Proceedings of the 2021 Conference on Empirical Methods in Natural Language Processing*, pp. 3045–3059, 2021.
- Leviathan, Y., Kalman, M., and Matias, Y. Fast inference from transformers via speculative decoding. In *International Conference on Machine Learning*, pp. 19274–19286. PMLR, 2023.
- Lewis, M., Liu, Y., Goyal, N., Ghazvininejad, M., Mohamed, A., Levy, O., Stoyanov, V., and Zettlemoyer, L. Bart: Denoising sequence-to-sequence pre-training for natural language generation, translation, and comprehension. *arXiv preprint arXiv:1910.13461*, 2019.
- Li, Y., Bubeck, S., Eldan, R., Del Giorno, A., Gunasekar, S., and Lee, Y. T. Textbooks are all you need ii: **phi-1.5** technical report. *arXiv preprint arXiv:2309.05463*, 2023.
- Liu, H., Dai, Z., So, D., and Le, Q. V. Pay attention to mlps. *Advances in Neural Information Processing Systems*, 34: 9204–9215, 2021.
- Liu, X., Xu, N., Chen, M., and Xiao, C. Autodan: Generating stealthy jailbreak prompts on aligned large language models. *arXiv preprint arXiv:2310.04451*, 2023a.
- Liu, Y., Yao, Y., Ton, J.-F., Zhang, X., Cheng, R. G. H., Klochkov, Y., Taufiq, M. F., and Li, H. Trustworthy llms: a survey and guideline for evaluating large language models’ alignment. *arXiv preprint arXiv:2308.05374*, 2023b.
- Maddison, C. J., Mnih, A., and Teh, Y. W. The concrete distribution: A continuous relaxation of discrete random variables. *arXiv preprint arXiv:1611.00712*, 2016.
- Madry, A., Makelov, A., Schmidt, L., Tsipras, D., and Vladu, A. Towards deep learning models resistant to adversarial attacks. *arXiv preprint arXiv:1706.06083*, 2017.
- Mökander, J., Schuett, J., Kirk, H. R., and Floridi, L. Auditing large language models: a three-layered approach. *AI and Ethics*, pp. 1–31, 2023.
- OpenAI. Gpt-4 technical report, 2023.
- Ouyang, L., Wu, J., Jiang, X., Almeida, D., Wainwright, C., Mishkin, P., Zhang, C., Agarwal, S., Slama, K., Ray, A., et al. Training language models to follow instructions with human feedback. *Advances in Neural Information Processing Systems*, 35:27730–27744, 2022.
- Park, P. S., Goldstein, S., O’Gara, A., Chen, M., and Hendrycks, D. Ai deception: A survey of examples, risks, and potential solutions. *arXiv preprint arXiv:2308.14752*, 2023.
- Pearson, K. X. on the criterion that a given system of deviations from the probable in the case of a correlated system of variables is such that it can be reasonably supposed to have arisen from random sampling. *The London, Edinburgh, and Dublin Philosophical Magazine and Journal of Science*, 50(302):157–175, 1900.

- Pincus, M. A monte carlo method for the approximate solution of certain types of constrained optimization problems. *Operations research*, 18(6):1225–1228, 1970.
- Qi, X., Zeng, Y., Xie, T., Chen, P.-Y., Jia, R., Mittal, P., and Henderson, P. Fine-tuning aligned language models compromises safety, even when users do not intend to! *arXiv preprint arXiv:2310.03693*, 2023.
- Radford, A., Wu, J., Child, R., Luan, D., Amodei, D., Sutskever, I., et al. Language models are unsupervised multitask learners. 2019.
- Rando, J. and Tramèr, F. Universal jailbreak backdoors from poisoned human feedback. *arXiv preprint arXiv:2311.14455*, 2023.
- Shayegani, E., Dong, Y., and Abu-Ghazaleh, N. Jailbreak in pieces: Compositional adversarial attacks on multi-modal language models. *arXiv preprint arXiv:2307.14539*, 2023.
- So, D., Le, Q., and Liang, C. The evolved transformer. In *International conference on machine learning*, pp. 5877–5886. PMLR, 2019.
- Stiennon, N., Ouyang, L., Wu, J., Ziegler, D., Lowe, R., Voss, C., Radford, A., Amodei, D., and Christiano, P. F. Learning to summarize with human feedback. *Advances in Neural Information Processing Systems*, 33: 3008–3021, 2020.
- Szegedy, C., Zaremba, W., Sutskever, I., Bruna, J., Erhan, D., Goodfellow, I., and Fergus, R. Intriguing properties of neural networks. *arXiv preprint arXiv:1312.6199*, 2013.
- Touvron, H., Martin, L., Stone, K., Albert, P., Almahairi, A., Babaei, Y., Bashlykov, N., Batra, S., Bhargava, P., Bhosale, S., et al. Llama 2: Open foundation and fine-tuned chat models. *arXiv preprint arXiv:2307.09288*, 2023.
- Toyer, S., Watkins, O., Mendes, E., Svegliato, J., Bailey, L., Wang, T., Ong, I., Elmaaroufi, K., Abbeel, P., Darrell, T., et al. Tensor trust: Interpretable prompt injection attacks from an online game. In *NeurIPS 2023 Workshop on Instruction Tuning and Instruction Following*, 2023.
- Wen, Y., Jain, N., Kirchenbauer, J., Goldblum, M., Geiping, J., and Goldstein, T. Hard prompts made easy: Gradient-based discrete optimization for prompt tuning and discovery. *arXiv preprint arXiv:2302.03668*, 2023.
- Xia, M., Gao, T., Zeng, Z., and Chen, D. Sheared llama: Accelerating language model pre-training via structured pruning. In *Workshop on Advancing Neural Network Training: Computational Efficiency, Scalability, and Resource Optimization (WANT@ NeurIPS 2023)*, 2023.
- Xu, C., Chern, S., Chern, E., Zhang, G., Wang, Z., Liu, R., Li, J., Fu, J., and Liu, P. Align on the fly: Adapting chatbot behavior to established norms. *arXiv preprint arXiv:2312.15907*, 2023.
- Yuan, W., Pang, R. Y., Cho, K., Sukhbaatar, S., Xu, J., and Weston, J. Self-rewarding language models. *arXiv preprint arXiv:2401.10020*, 2024.
- Yuan, Y., Jiao, W., Wang, W., Huang, J.-t., He, P., Shi, S., and Tu, Z. Gpt-4 is too smart to be safe: Stealthy chat with llms via cipher. *arXiv preprint arXiv:2308.06463*, 2023.
- Zar, J. H. Spearman rank correlation. *Encyclopedia of biostatistics*, 7, 2005.
- Zhang, P., Zeng, G., Wang, T., and Lu, W. Tinyllama: An open-source small language model. *arXiv preprint arXiv:2401.02385*, 2024.
- Zheng, L., Chiang, W.-L., Sheng, Y., Zhuang, S., Wu, Z., Zhuang, Y., Lin, Z., Li, Z., Li, D., Xing, E., et al. Judging llm-as-a-judge with mt-bench and chatbot arena. *arXiv preprint arXiv:2306.05685*, 2023.
- Zou, A., Wang, Z., Kolter, J. Z., and Fredrikson, M. Universal and transferable adversarial attacks on aligned language models. *arXiv preprint arXiv:2307.15043*, 2023.

A. Implementation

The following code shows the core implementation of probe sampling using PyTorch. As seen in the code, the algorithm is relatively easy to use.

```
def draft_model_all(args):
    draft_model.loss(control_cands)

    queue.put('draft':loss_small)

def target_model_probe(args):
    probe_index = random.sample(range(512), 512/16)
    probe_control_cands = control_cands[probe_index]
    target_model.loss(probe_control_cands)

    queue.put('target':[loss_large_probe, probe_index])

# Parallellly Calculate Loss on Batch and Probe Set
args=(control_cands, batch_size, queue)
threading.Thread(target=draft_model_all, args=args)
threading.Thread(target=target_model_probe, args=args)

# Calculate Agreement Score
cor = spearmanr(loss_small[probe_index], large_loss_probe)

# Target Model Test on Filtered Set
filtered_size = int((1 - cor) * 512/8)
indices = topk(loss_small, k=filtered_size, largest=False)
filtered_control_cands = control_cands[indices]
target_model.loss(filtered_control_cands)

# Return Lowest Loss Candidate
return [large_loss_probe, filtered_control_cands].lowest()
```
